SciGlass Samples Tests 2022

August 5, 2022

Yuwei Zhu and Carlos Munoz Camacho
IJCLab

Contents

Abstract

We report on the tests of 10 samples of SciGlass received from CUA in June 2022. The tests mainly consist of transmittance measurements, light yield measurements, and radiation hardness.

1 Visual aspect

We received ten samples of SciGlass from CUA which are labeled CUA2022-2_1, CUA2022-2_2, CUA2022-2_3, CUA2022-2_4, CUA2022-2_5, CUA2022-5_1, CUA2022-5_2, CUA2022-5_3, CUA2022-5_4, and CUA2022-5_5, as illustrated in Figure 1.

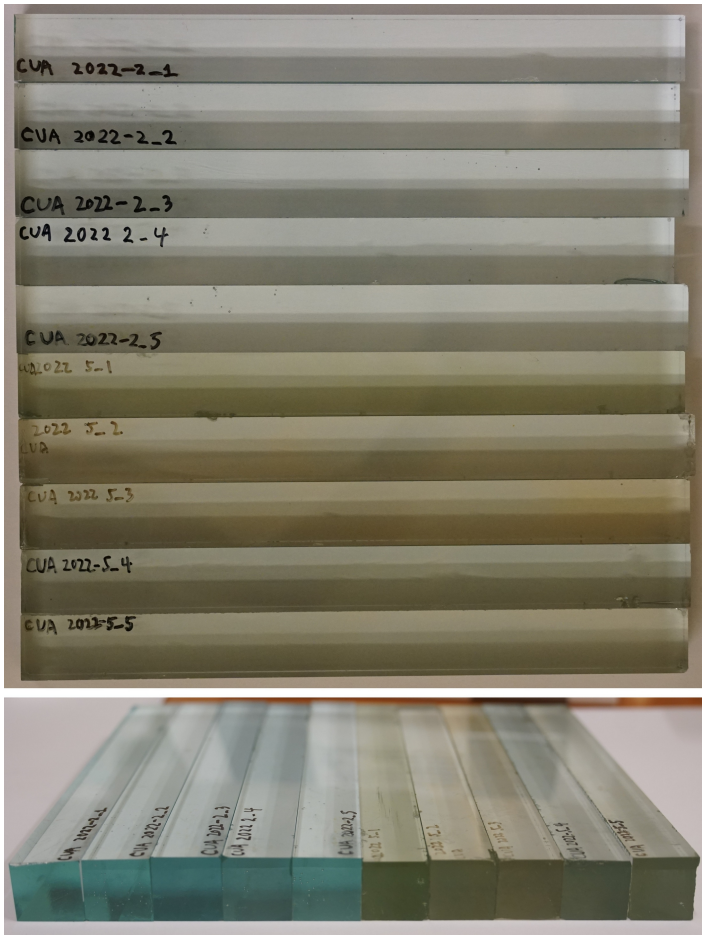

Figure 1: Ten SciGlass samples

These samples contain two series (CUA2022-2_X and CUA2022-5_X). The color of series CUA2022-5_X are more greenish than series CUA2022-2_X, as presented in Figures 2 and 3.

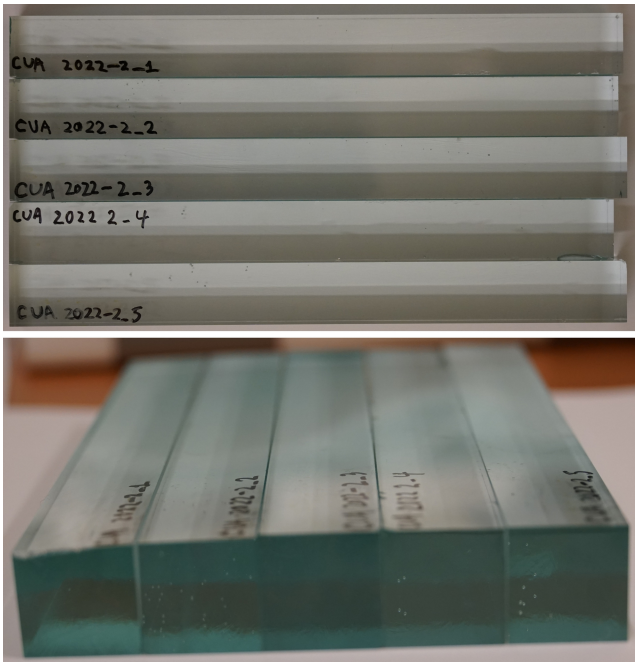

Figure 2: Five SciGlass samples of CUA2022-2_X series

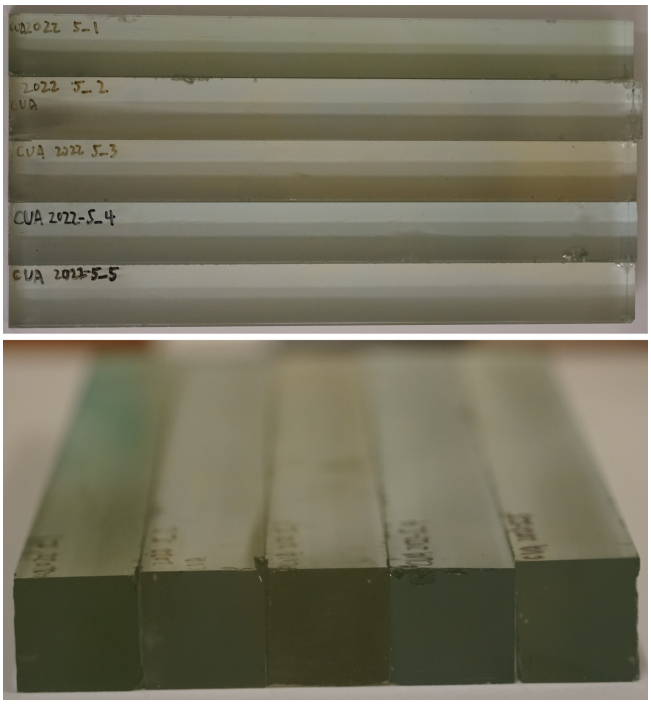

Figure 3: Five SciGlass samples of CUA2022-5_X series

The samples are about 20 cm (≈ $7X_0$) long. The length of the longest sample is 20.15 cm, and the shortest is 19.55 cm. Compared with the samples produced last year (the face is not a perfect square), the cross sections of the current samples are a square of about 2.0 × 2.0 cm^2. Some samples have a rectangular form of 1.95 × 1.9 cm^2. The size of ten SciGlass samples are listed in Table 1.1. Compared with the samples produced last year, the surfaces of the current samples are polished. However, there are still some small bubbles in their bulks. The edges and corners of several samples are worn and bumped. The details of these samples are presented in Figure 4.

	2_1	2_2	2_3	2_4	2_5	5_1	5_2	5_3	5_4	5_5
Length (cm)	1.95	1.92	2.00	2.00	2.00	1.92	1.95	1.92	1.95	1.95
Width (cm)	1.85	1.95	2.00	2.00	2.00	1.87	1.90	1.90	1.90	1.95
Height (cm)	19.90	19.70	20.00	19.55	19.95	19.85	20.10	20.00	20.00	19.90

Table 1.1 – Size of ten SciGlass samples

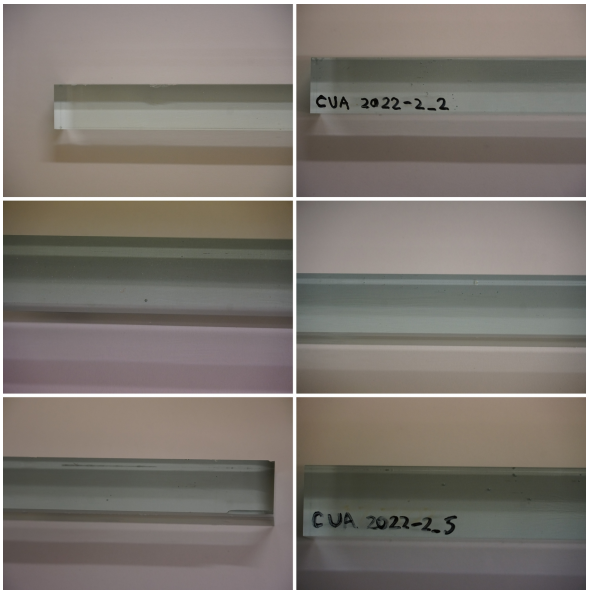

Figure 4: Details of the SciGlass samples

2 Transmittance measurements

The transmittance of the samples was measured using a Perkin-Elmer Lambda 850 spectrophotometer. Each sample was measured longitudinally, with each face and each side containing eight different orientations. The transmittance of each orientation is measured from 750 nm to 350 nm with a data interval of 1 nm. The transmittance results for all the samples are presented in Figures 5 to 15.

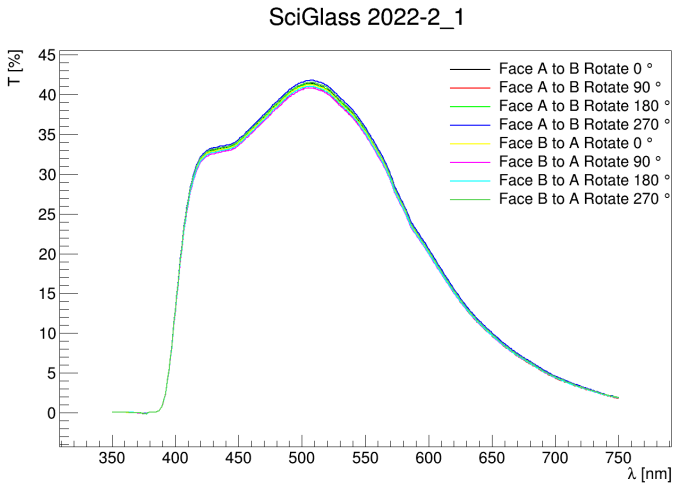

Figure 5: Transmittance of sample CUA2022-2_1

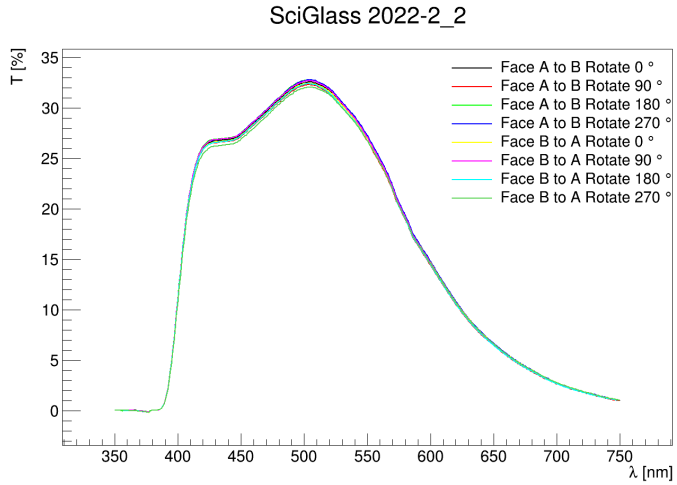

Figure 6: Transmittance of sample CUA2022-2_2

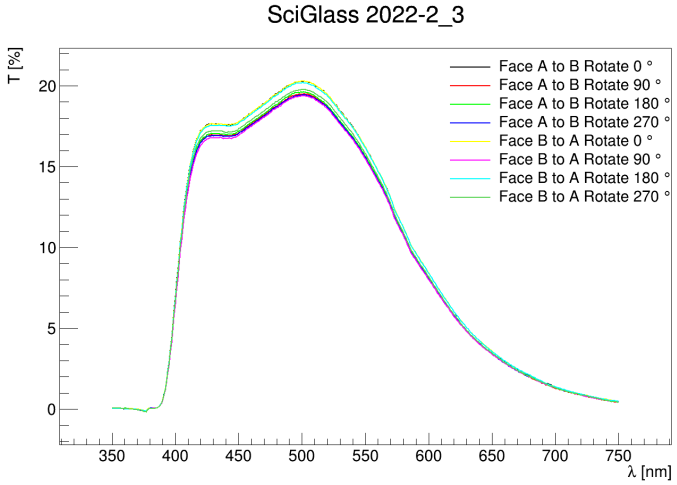

Figure 7: Transmittance of sample CUA2022-2_3

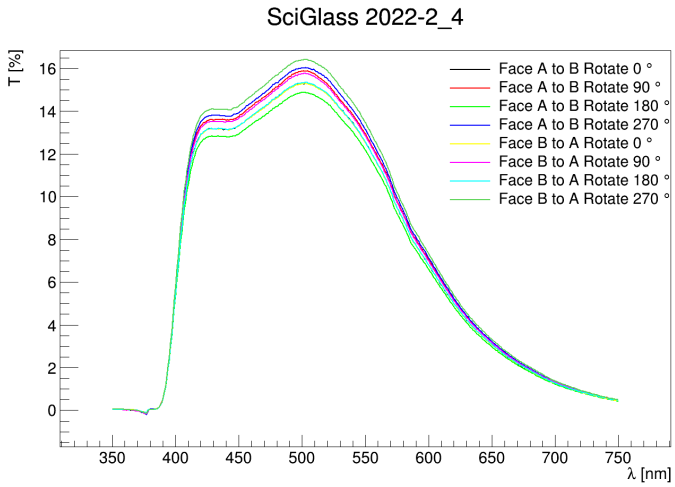

Figure 8: Transmittance of sample CUA2022-2_4

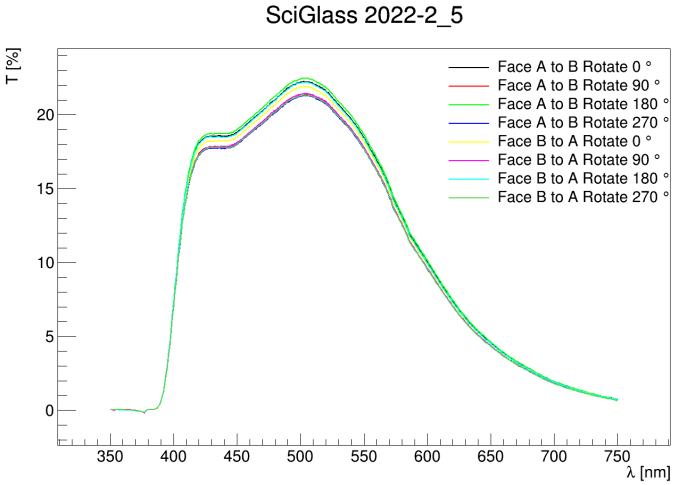

Figure 9: Transmittance of sample CUA2022-2_5

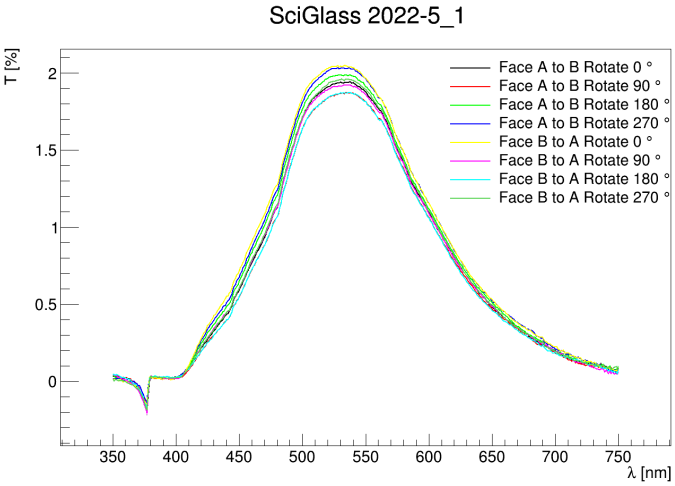

Figure 10: Transmittance of sample CUA2022-5_1

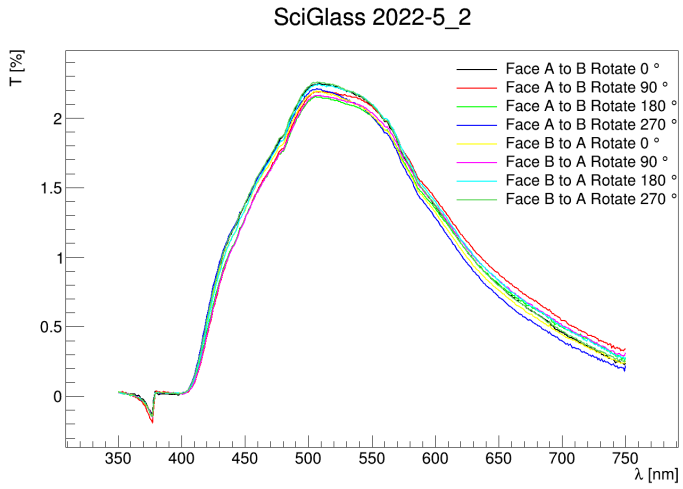

Figure 11: Transmittance of sample CUA2022-5_2

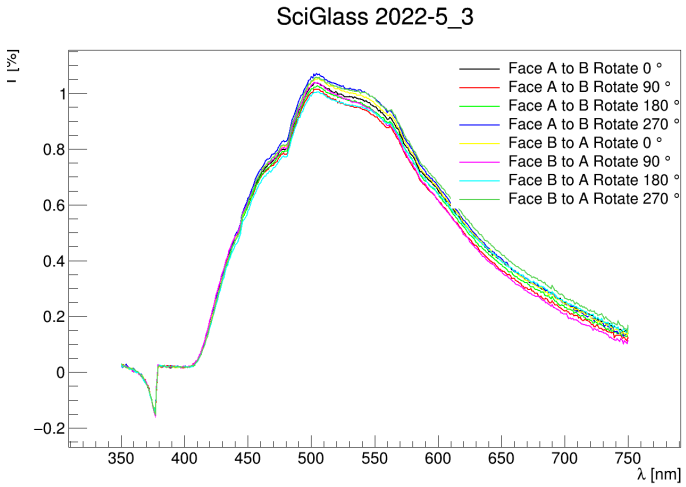

Figure 12: Transmittance of sample CUA2022-5_3

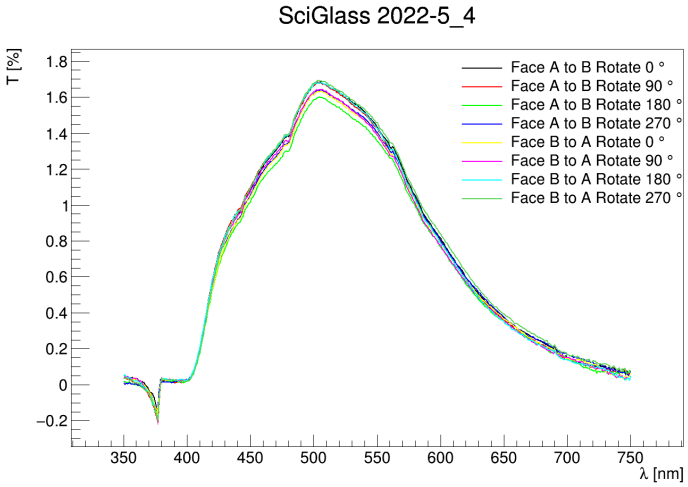

Figure 13: Transmittance of sample CUA2022-5_4

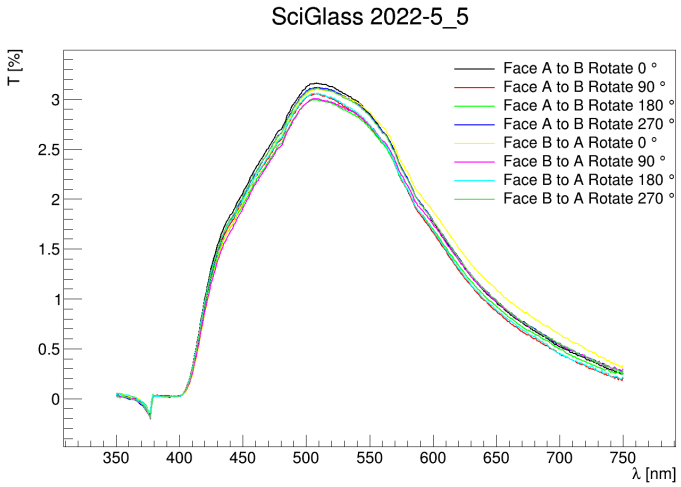

Figure 14: Transmittance of sample CUA2022-5_5

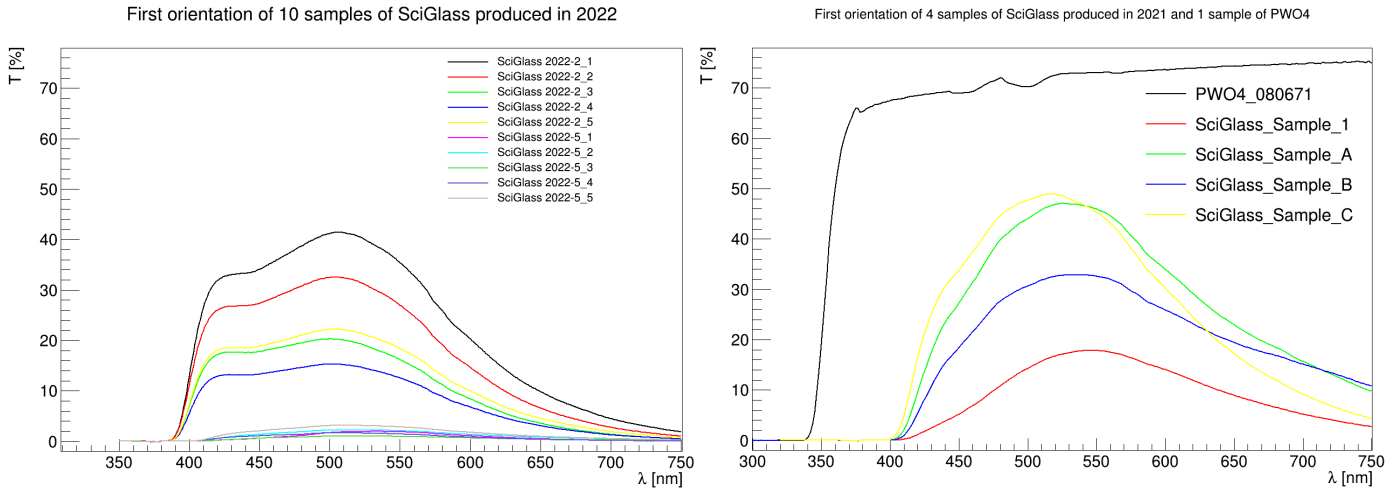

Figure 15: Transmittance of ten SciGlass samples produced in 2022 (left figure), one PWO4, and four SciGlass samples produced in 2021 (right figure) for first orientation

The transmittance varies considerably from sample to sample (from 40% to 1%). Compared with the series CUA2022-5_X, all the samples from the series CUA2022-2_X have better transmittance, as expected by visual inspection. However, compared with the same procedure by Noémie Pilleux for four 20 cm-long SciGlass samples produced last year ([2]), the transmittance of the current samples are much lower, especially for the series CUA2022-5_X whose transmittance is only a few percent. The maximum transmittance values are within a limited range of wavelengths. In particular, at 450 nm (the peak of the emission spectrum, according to Fig. 11.51 of the EIC Yellow Report [1]) the transmittance are of 34.1% for sample CUA2022-2_1, 27.2% for sample CUA2022-2_2, 17.7% for sample CUA2022-2_3, 13.3% for sample CUA2022-2_4, 18.7% for sample CUA2022-2_5, 0.6% for sample CUA2022-5_1, 1.4% for sample

CUA2022-5_2, 0.6% for sample CUA2022-5_3, 1.1% for sample CUA2022-5_4, and 2.1% for sample CUA2022-5_5. For reference, the transmittance of the PbWO4 crystals that we measured last year are about 70% between 450 nm and 800 nm.

3 Light yield measurements

The light yield (LY) of five samples in series CUA2022-2_X were measured. For the series CUA2022-5_X, due to their very low light transmittance (< 2%), the light yield cannot be measured with the current method. The setup is shown in Figure 16. A sample (wrapped in reflective paper) is coupled using optical grease to a photo-multiplier tube (PMT), whose model number is HAMAMATSU R2083. Then, the PMT output signals are read by a waveform digitizer (CAEN DT5730_1204). The sample and the PM are placed in a black box. A radioactive source is placed inside the same black box on the sample and can be moved along the sample. The LY of the five samples were studied as a function of the position of the source, which corresponds to the distance between the outer edge of the source towards the PMT and the junction between the PMT and the sample. Position 0 cm corresponds to the source outer edge being aligned with the junction, and position 18 cm to the source outer edge at the end of the sample.

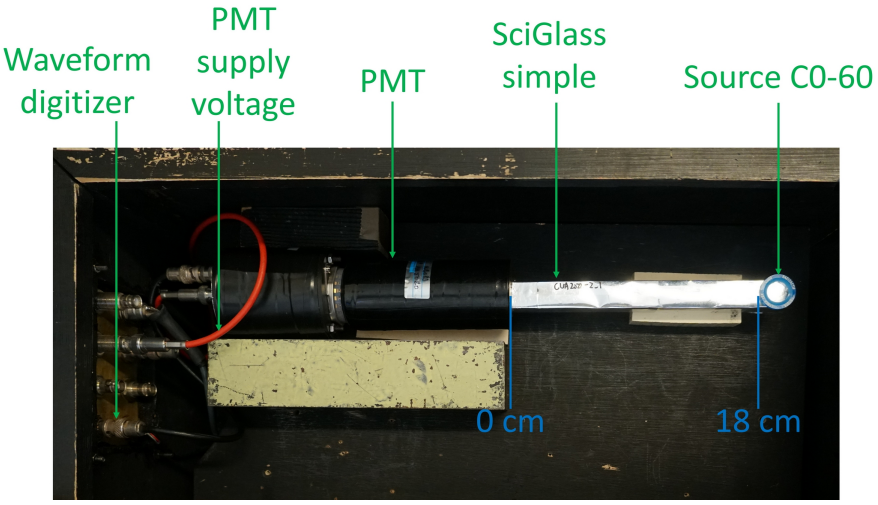

Figure 16: Experimental setup of the light yield measurement for SciGlass samples

For each sample and each position of the source, the acquisition time and parameters were the same. Two groups of data are recorded for each source position: the

background noise data was stored without a radioactive source, and a source of ^{60}Co was then placed on the sample. The background was then subtracted from the signal. An example of a measurement for sample CUA2022-2_1 at position 0 cm is presented in Figure 17. After the subtraction, the distribution was fitted with a double Gaussian function. For each sample and each position, the energy spectrum after the background subtraction are shown in Figures 18 to 22.

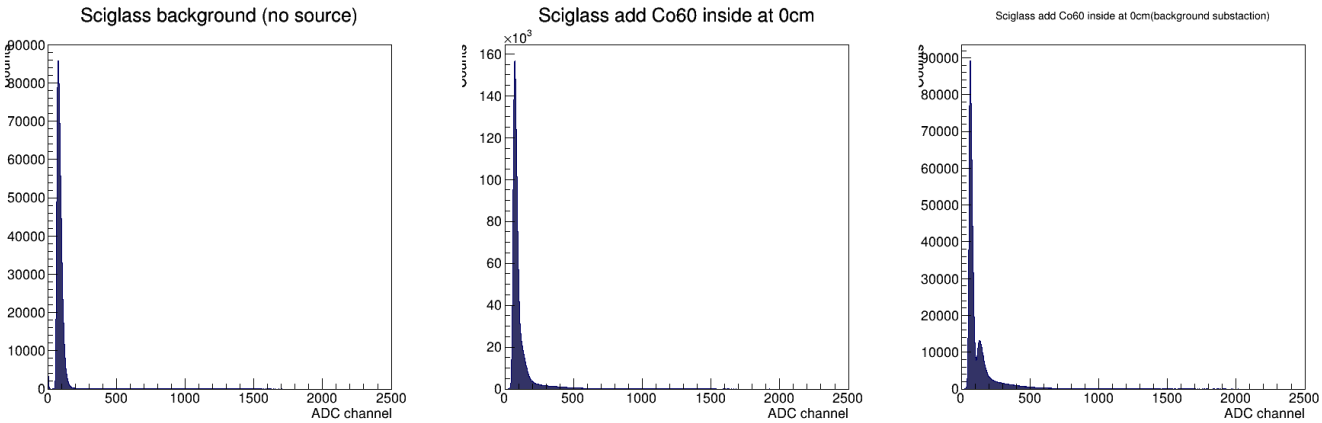

Figure 17: Example of measurement for sample CUA2022-2_1 at position 0 cm

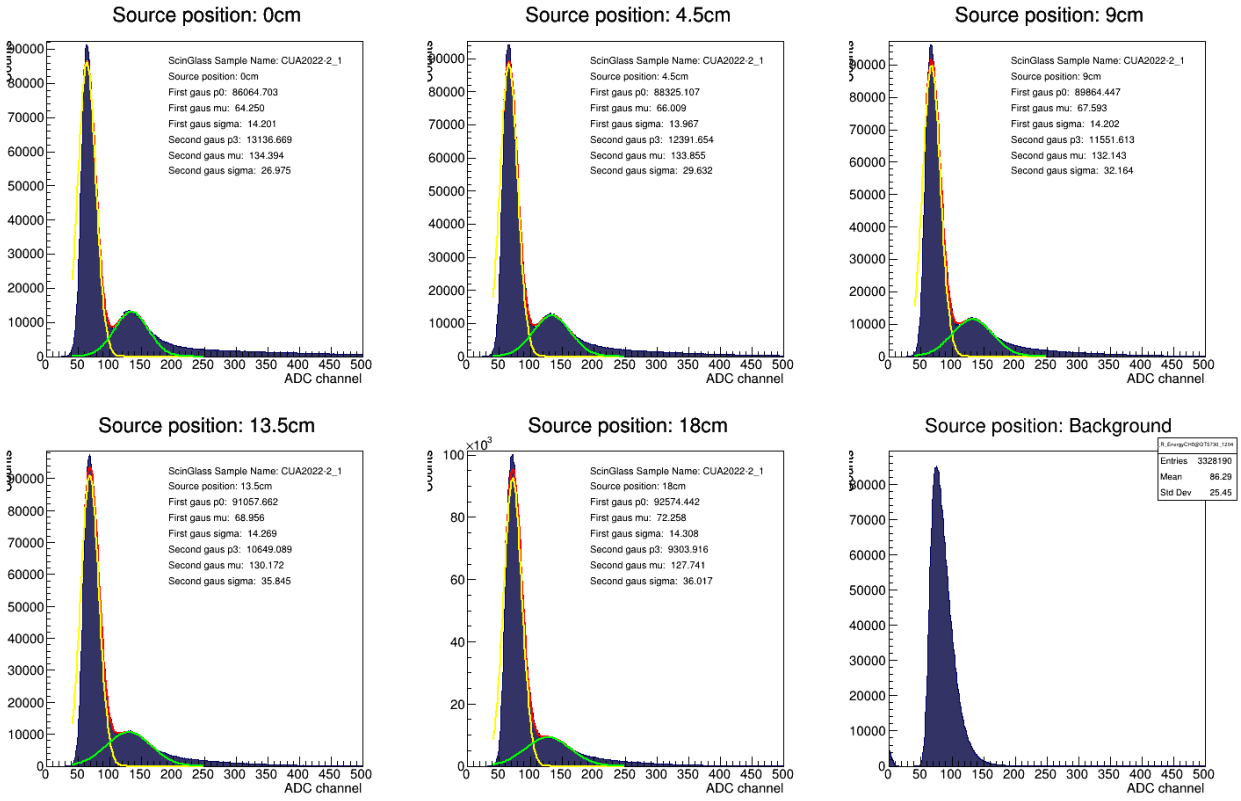

Figure 18: Background subtraction energy spectrum of CUA2022-2_1 at different positions

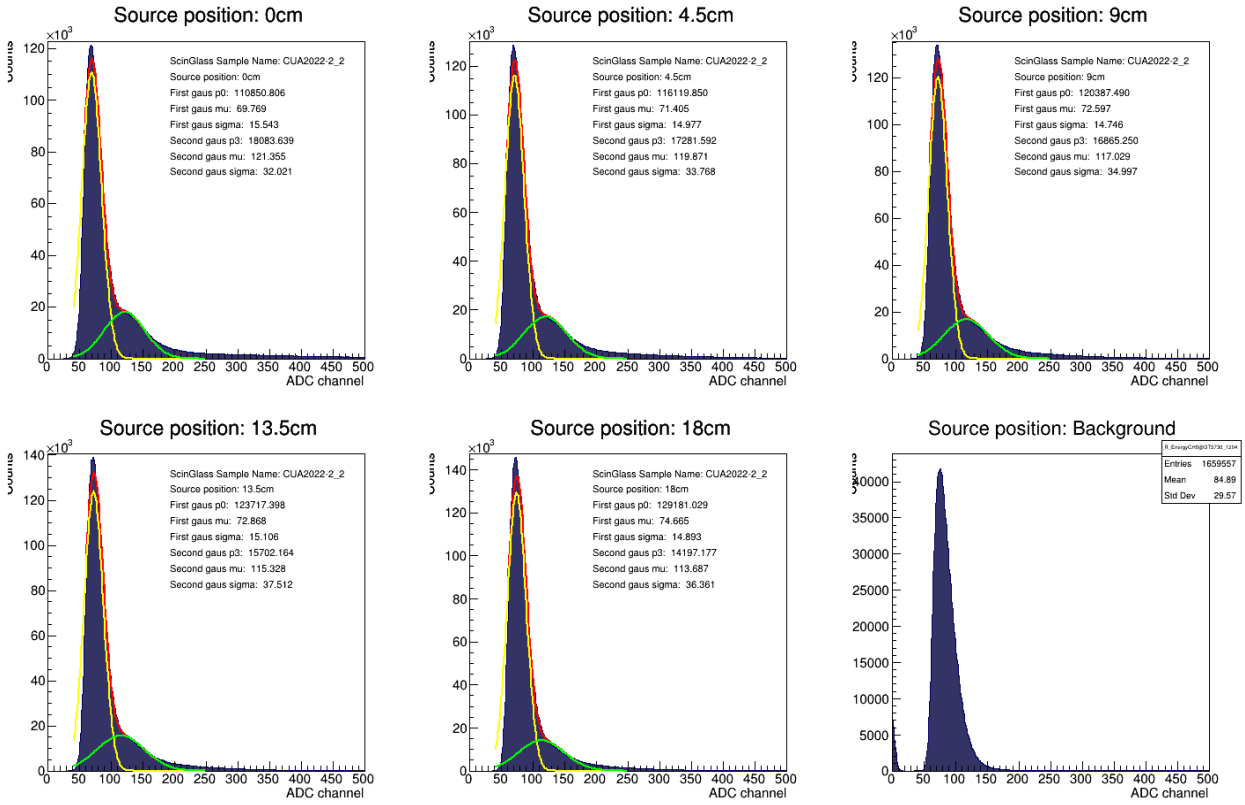

Figure 19: Background subtraction energy spectrum of CUA2022-2_2 at different positions

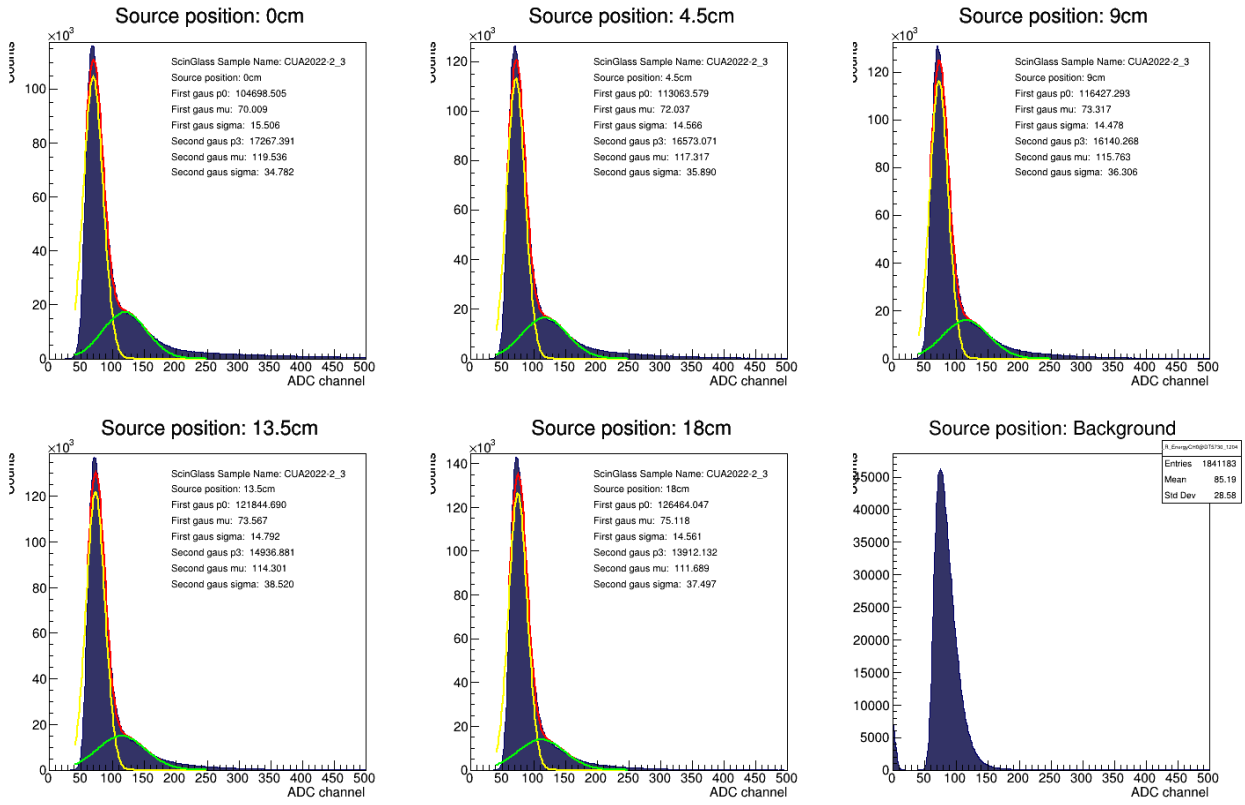

Figure 20: Background subtraction energy spectrum of CUA2022-2_3 at different positions

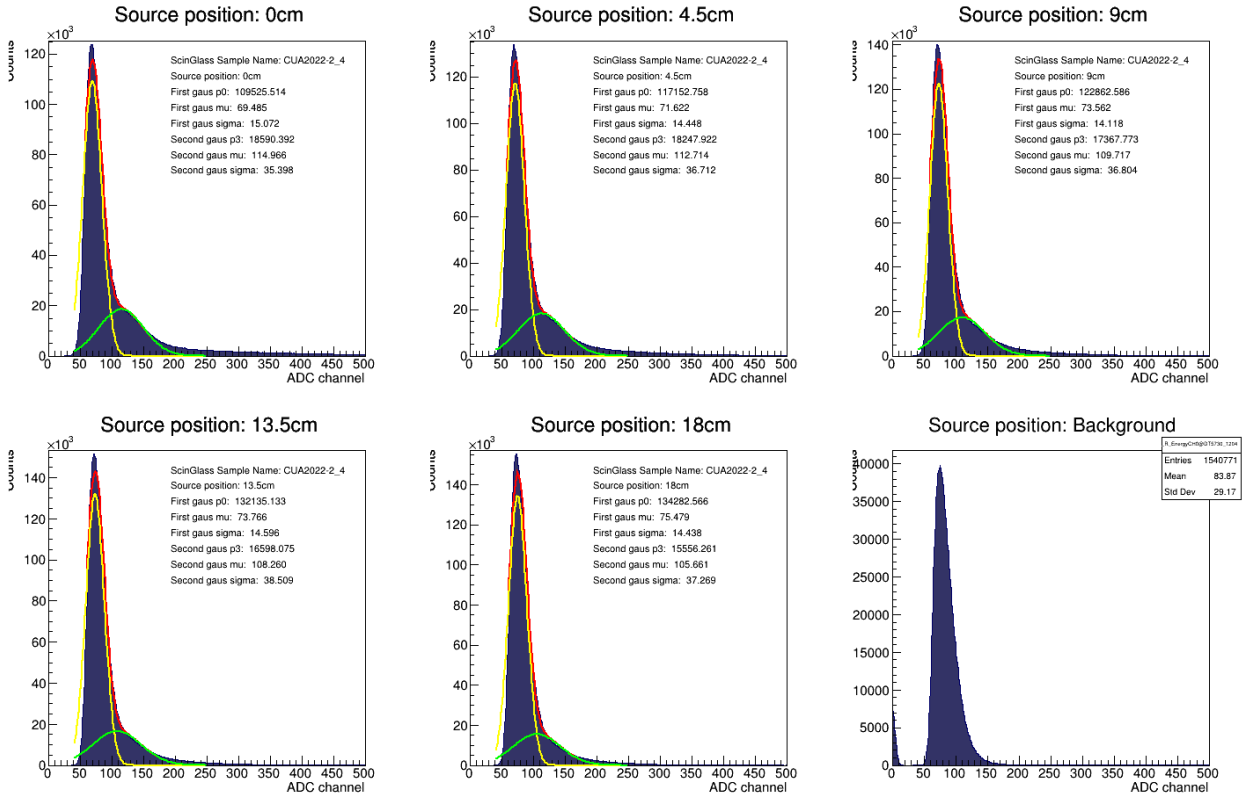

Figure 21: Background subtraction energy spectrum of CUA2022-2_4 at different positions

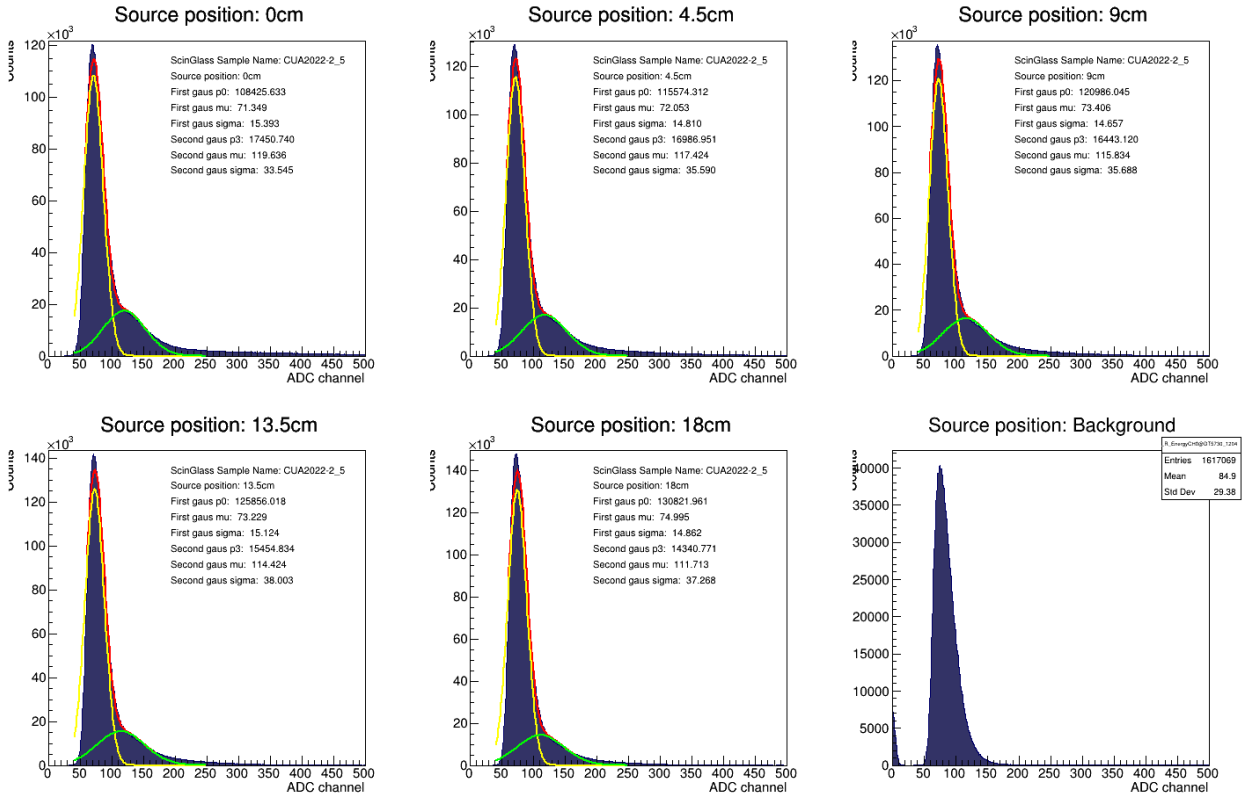

Figure 22: Background subtraction energy spectrum of CUA2022-2_5 at different positions

The mean of the second Gaussian fit function is used to compute the number of photo-electron (p.e) per MeV received by the PMT, which relies on the single p.e spectrum of the PM (which was measured).

$$\frac{p.e}{MeV} = \frac{\text{second Gaussian mean ADC value}}{\text{ADC interval between two single p.e peaks} \times \text{mean energy of the radiation source}} \quad (1)$$

The gain of the PMT was measured to be 1.67×10^{6} , and the corresponding ADC interval between two single p.e peaks is 53.5. Since ^{60}Co emits at two energies that cannot be distinguished with our experiment (1.173 MeV and 1.332 MeV), we use the mean energy of 1.253 MeV in the formula. Finally, the light yield is computed as :

$$\frac{\gamma}{MeV} = \frac{p.e/MeV}{QE \times T \times \text{fraction of reflected and scattered photons}} \quad (2)$$

For the HAMAMATSU R2083 PMT, the quantum efficiency QE is about 0.25 at 450 nm, as presented in Figure 23. We used a fraction of reflected and scattered photons (to account for photons that escaped and did not enter the PMT) of 0.9. The transmittance T is taken from our measurement at 450 nm.

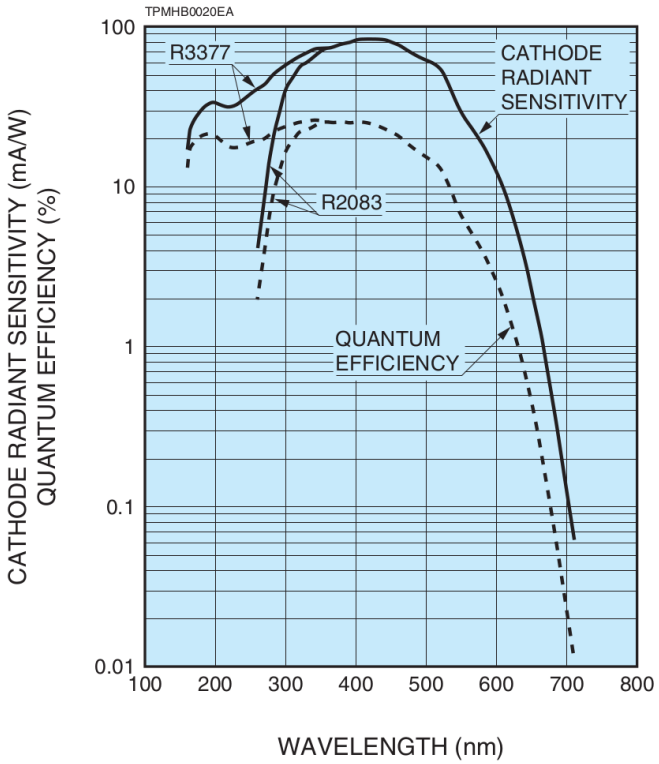

Figure 23: Typical spectral response

For each sample, the number of p-e/MeV received by the PMT and light yield as a function of the position of the source are presented in Figures 24 and 25.

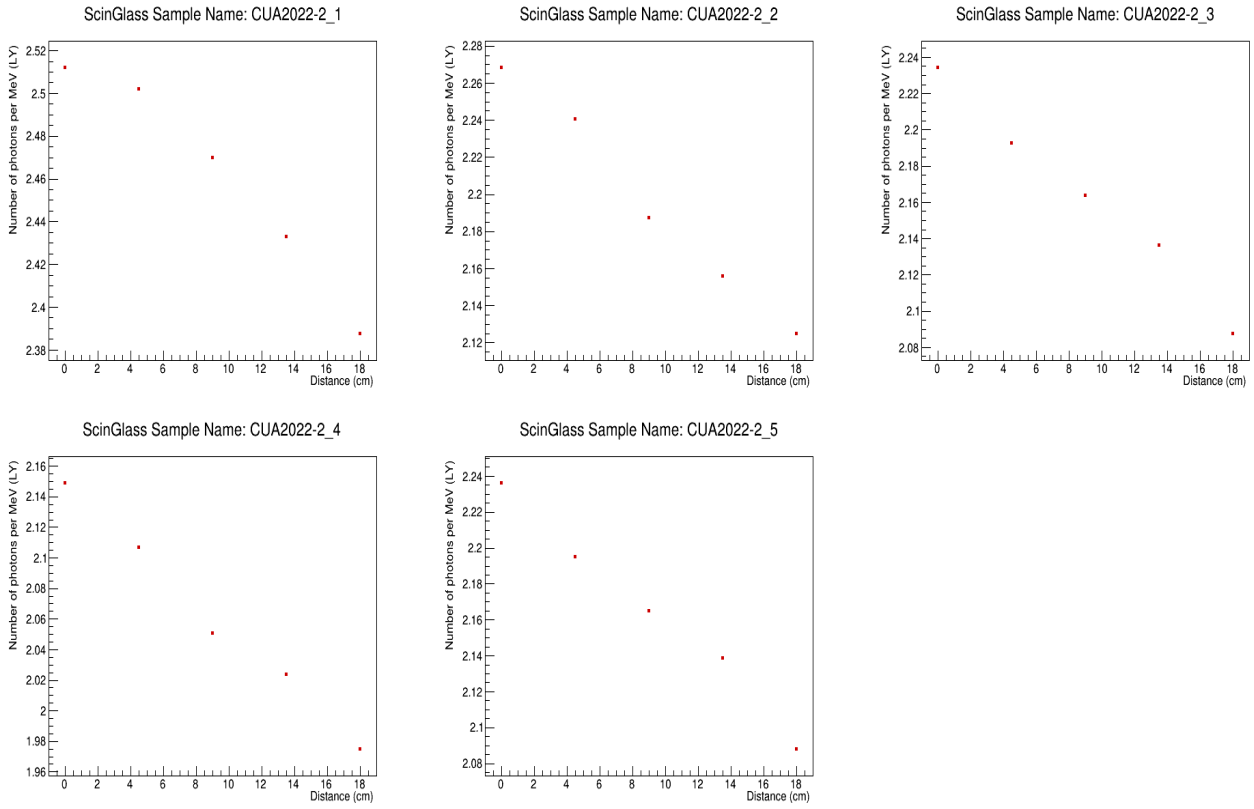

Figure 24: Number of p-e/MeV as a function of the source position for CUA2022-2_X series

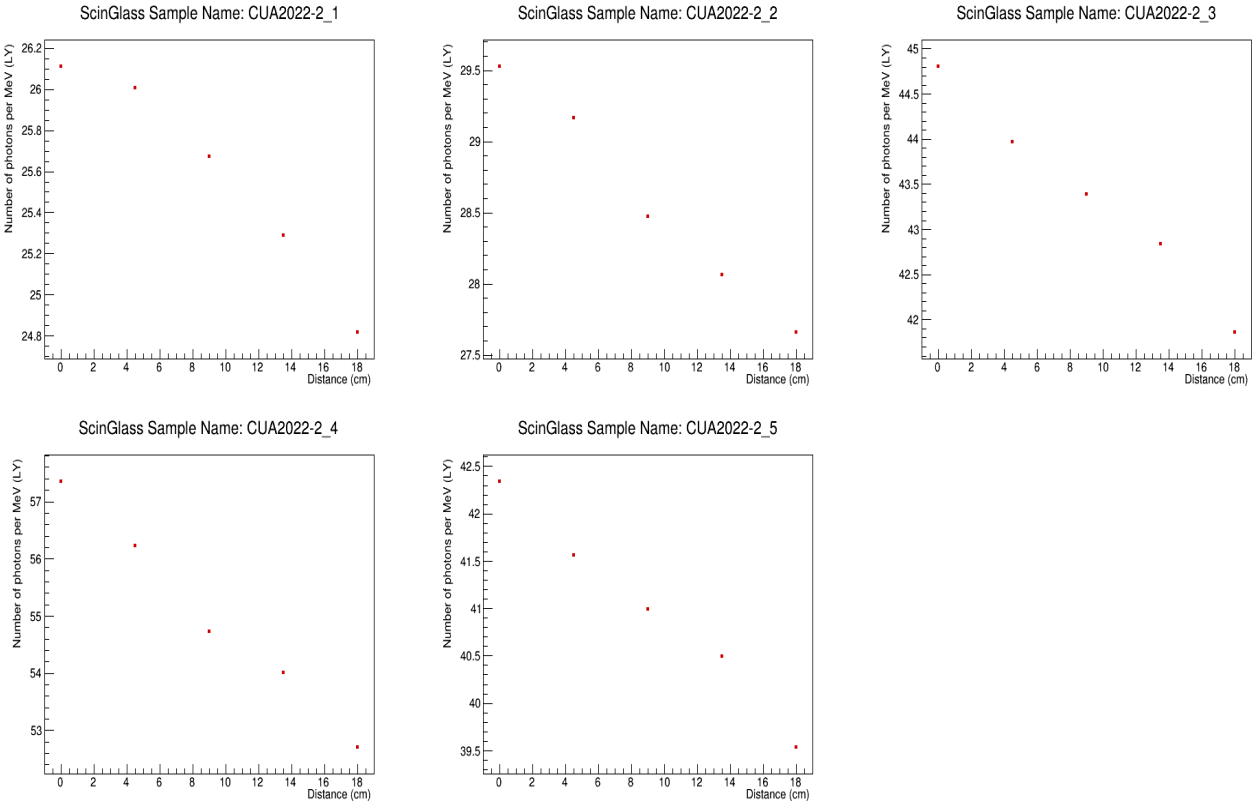

Figure 25: Light yield as a function of the source position for CUA2022-2_X series

Comparing the results of the LY or the number of p.e/MeV received by the PMT between a distance of 0 cm and a distance of 18 cm, the value drops by 4.98% for sample CUA2022-2_1, 6.10% for sample CUA2022-2_2, 6.47% for sample CUA2022-2_3, 8.01% for sample CUA2022-2_4, and 6.61% for sample CUA2022-2_5. Compared with the samples produced last year [2], the light yield of the current samples are at least two times lower.

4 Radiation hardness

The samples were irradiated to test their radiation hardness. They were irradiated under a dose of 30Gy (which is an estimation of the dose that could be received in one year at the EIC) at a rate of 1Gy/min. Their transmittance with a fixed orientation of the sample was measured after the irradiation and compared to the one before irradiation. After that, the samples were left for 11 days, and their transmittance was measured. Finally, the samples were subjected to thermal annealing. The transmittance of all the samples before, right after, 11 days after irradiation, and after thermal annealing are shown in Figures 26 to 36. The value of $dk = \frac{\ln\left(T_{before\,irradiation} / T_{after\,irradiation}\right)}{d}$ (where d = 0.2 m is the average length of the sample) as a function of the wavelength are also presented.

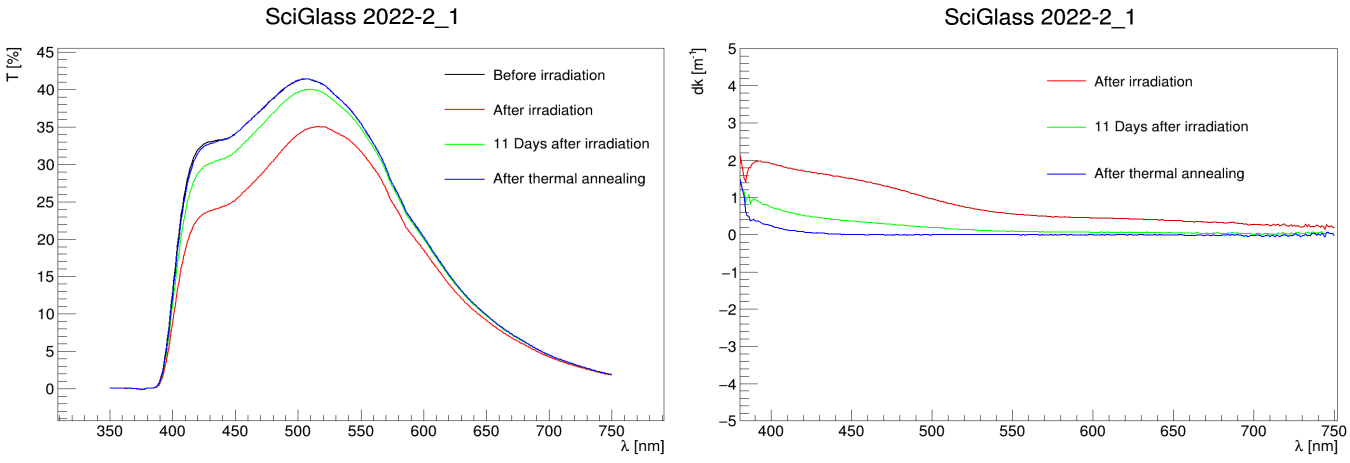

Figure 26: Transmittance of sample CUA2022-2_1 before, right after, 11 days after irradiation, and after thermal annealing

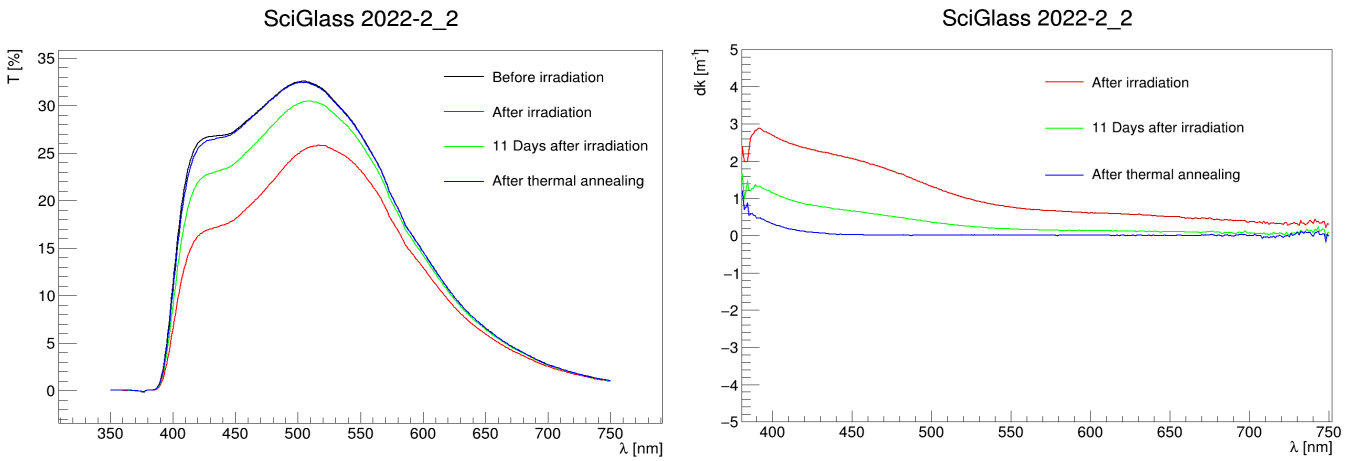

Figure 27: Transmittance of sample CUA2022-2_2 before, right after, 11 days after irradiation, and after thermal annealing

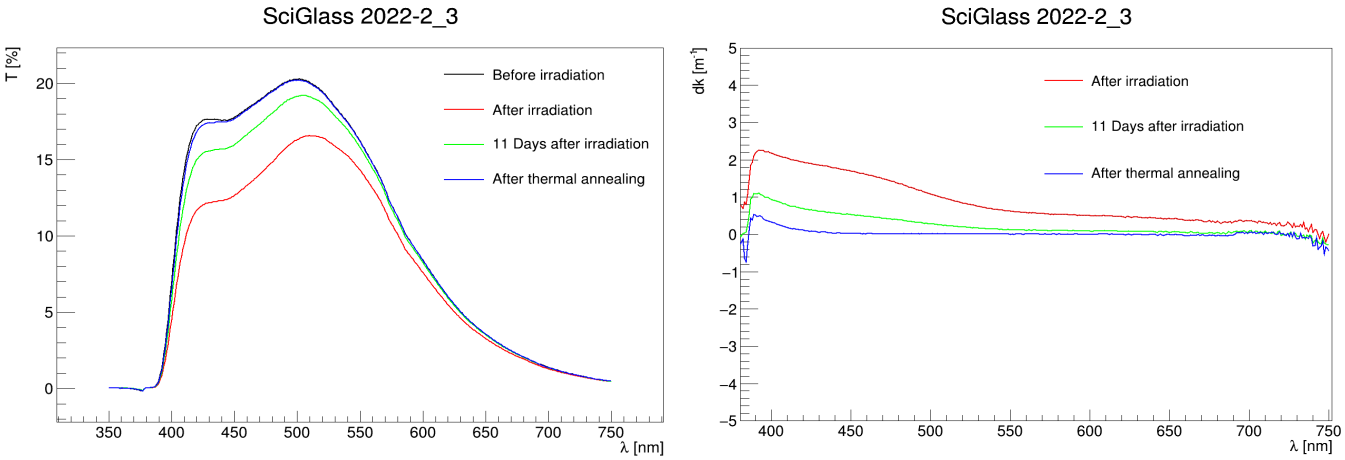

Figure 28: Transmittance of sample CUA2022-2_3 before, right after, 11 days after irradiation, and after thermal annealing

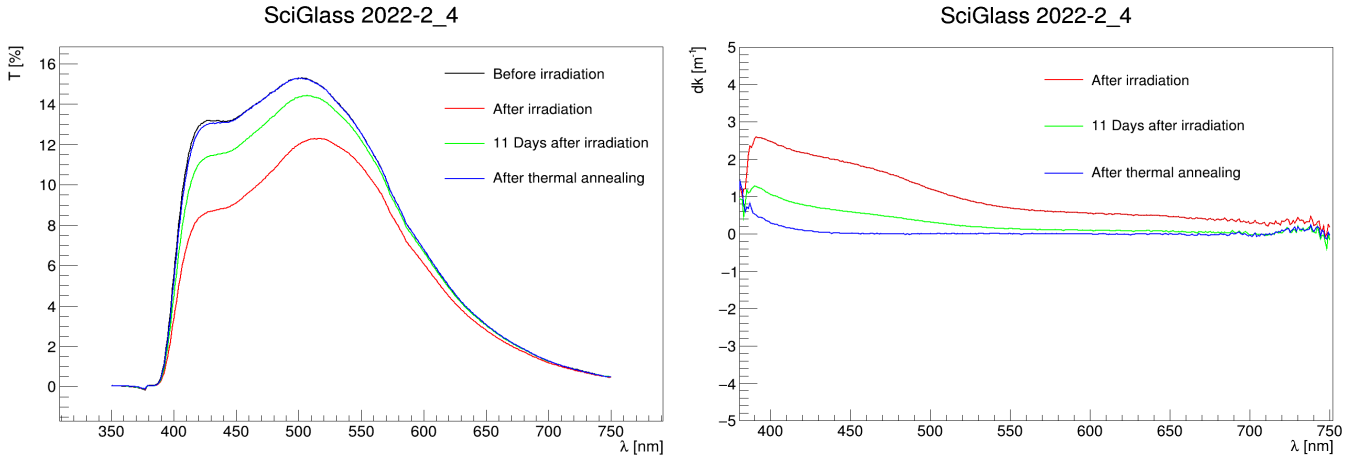

Figure 29: Transmittance of sample CUA2022-2_4 before, right after, 11 days after irradiation, and after thermal annealing

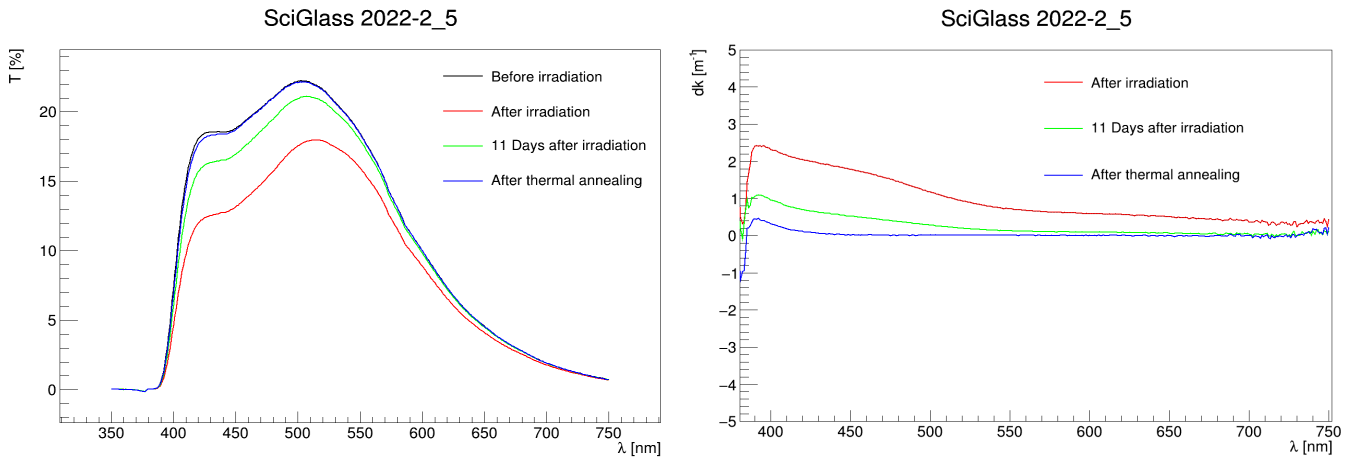

Figure 30: Transmittance of sample CUA2022-2_5 before, right after, 11 days after irradiation, and after thermal annealing

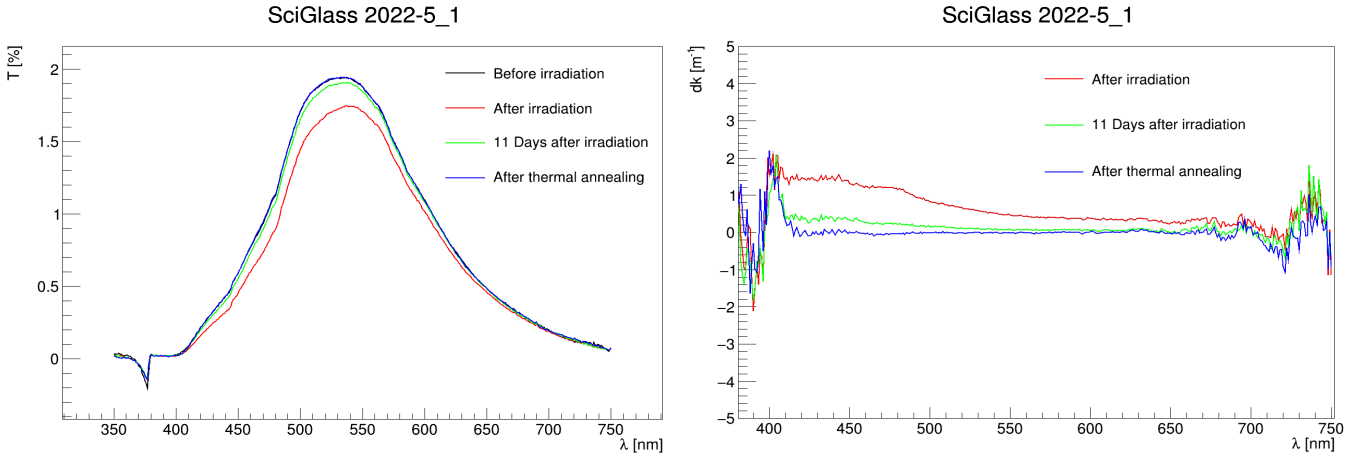

Figure 31: Transmittance of sample CUA2022-5_1 before, right after, 11 days after irradiation, and after thermal annealing

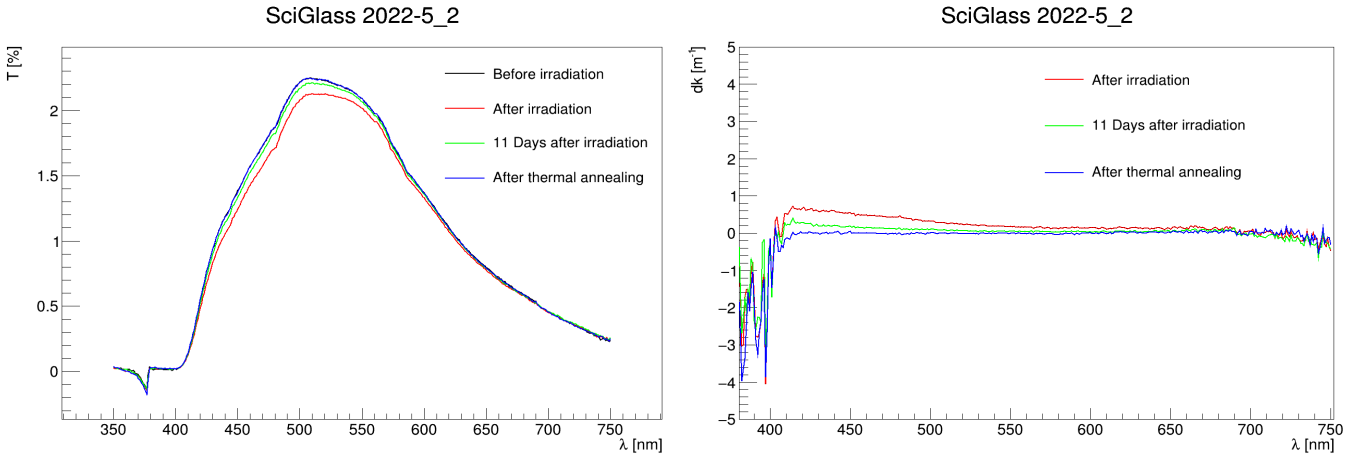

Figure 32: Transmittance of sample CUA2022-5_2 before, right after, 11 days after irradiation, and after thermal annealing

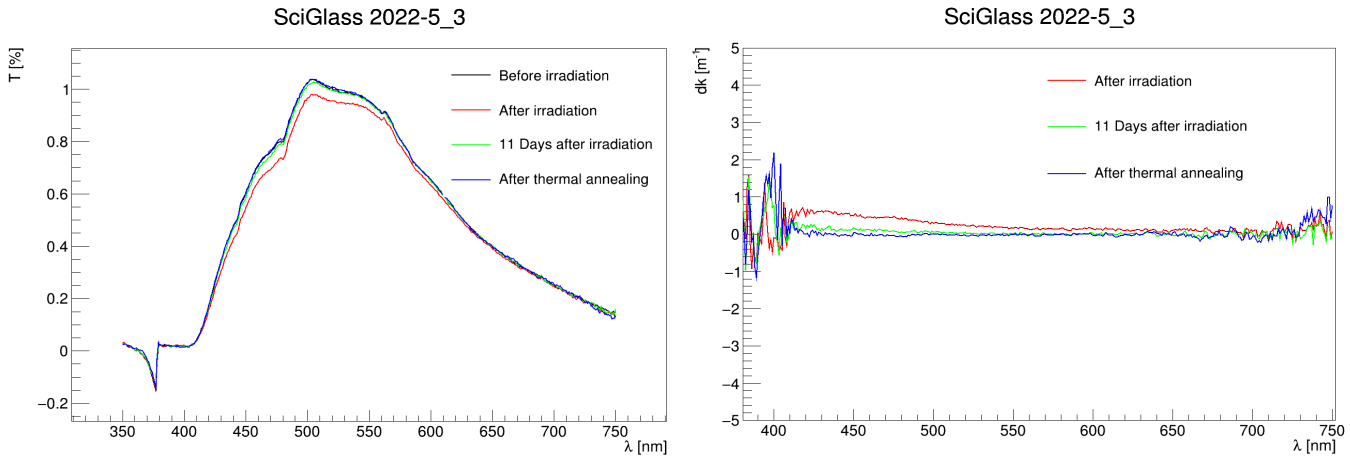

Figure 33: Transmittance of sample CUA2022-5_3 before, right after, 11 days after irradiation, and after thermal annealing

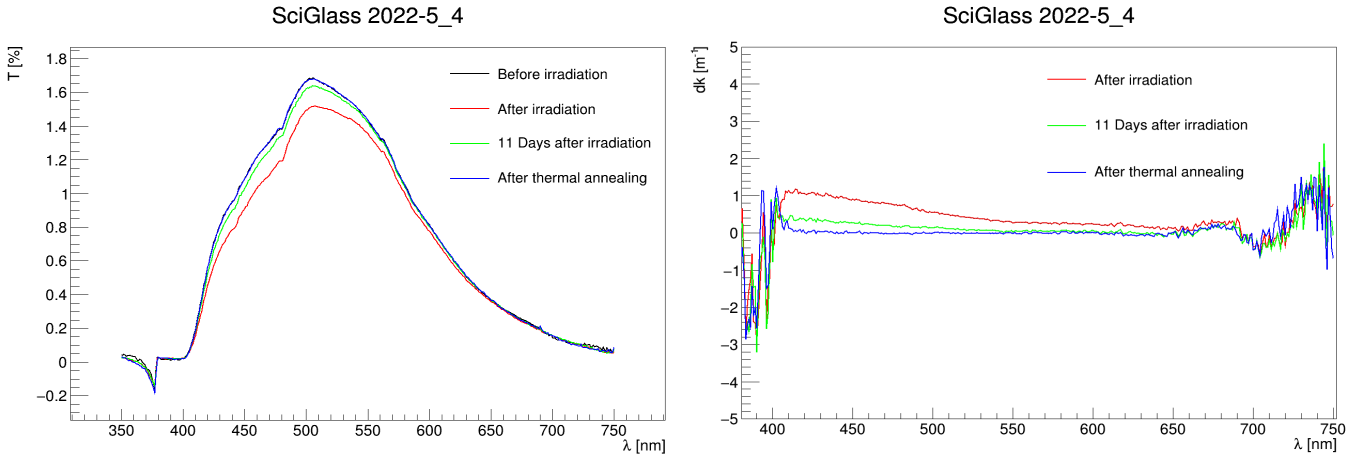

Figure 34: Transmittance of sample CUA2022-5_4 before, right after, 11 days after irradiation, and after thermal annealing

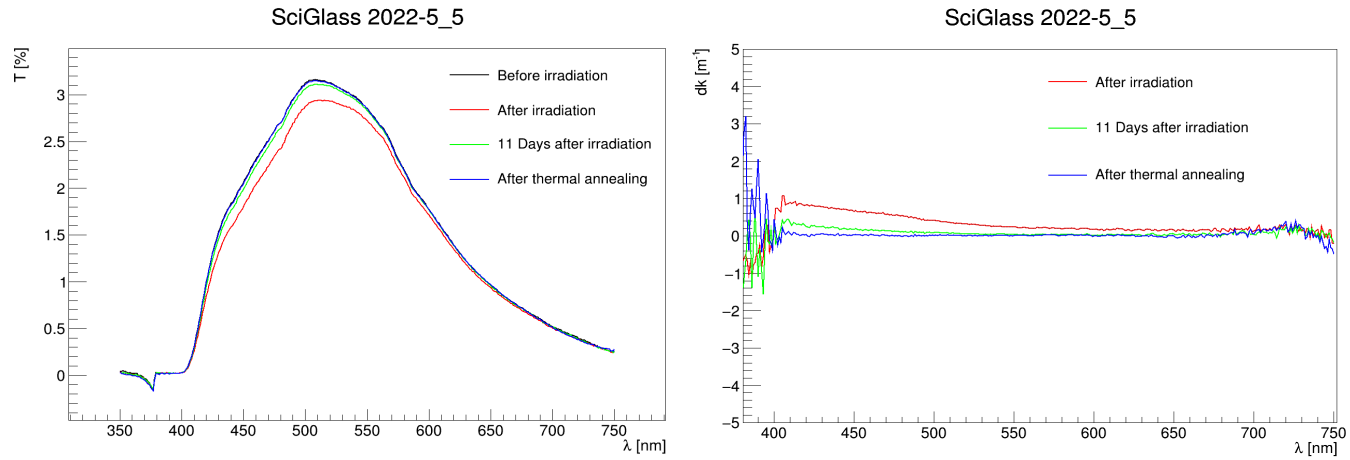

Figure 35: Transmittance of sample CUA2022-5_5 before, right after, 11 days after irradiation, and after thermal annealing

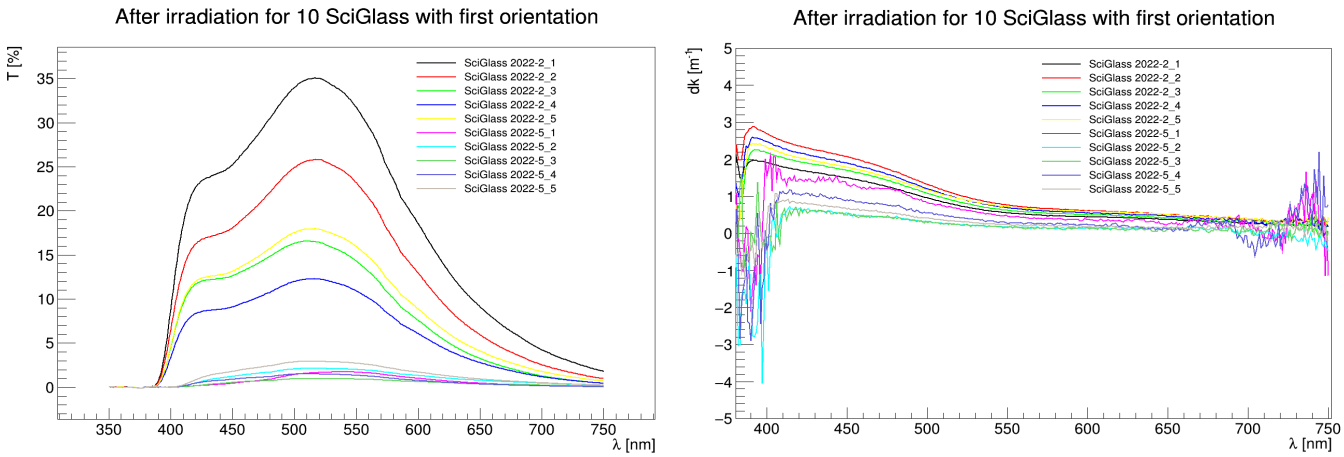

Figure 36: Transmittance of all the sample with first orientation right after irradiation

It is found that the radiation damage of the samples with the series CUA2022-2_X are more significant compared with the series CUA2022-5_X. Besides, the transmittance did not recover naturally to the per-irradiation levels even after several days. Therefore, the sample underwent thermal annealing. Finally, almost all the samples fully recovered after high-temperature treatment. Compared with the samples produced last year [2], the radiation damage of the current samples are more significant, especially for the series CUA2022-2_X.

References

[1] The EIC Users Group. *Science Requirements and Detector Concepts for the Electron-Ion Collider: EIC Yellow Report.* 2021.

[2] Carlos Munoz Camacho and Noémie Pilleux. *SciGlass samples tests.* 2021.